A thermodynamically self-consistent damage equation for grain size evolution during dynamic recrystallization

Antoine Rozel,[1] Yanick Ricard[1] and David Bercovici[2]

[1]*Laboratoire des Sciences de la Terre, CNRS, Université de Lyon 1, ENSL 46 allée d'Italie, F-69364 Lyon, Cedex 07, France. E-mail: antoinerozel@yahoo.fr*
[2]*Department of Geology and Geophysics, Yale University, New Haven, Connecticut, USA*

SUMMARY

We employ basic non-equilibrium thermodynamics to propose a general equation for the mean grain size evolution in a deforming medium, under the assumption that the whole grain size distribution remains self-similar. We show that the grain size reduction is controlled by the rate of mechanical dissipation in agreement with recent findings. Our formalism is self consistent with mass and energy conservation laws and allows a mixed rheology. As an example, we consider the case where the grain size distribution is lognormal, as is often experimentally observed. This distribution can be used to compute both the kinetics of diffusion between grains and of dynamic recrystallization. The experimentally deduced kinetics of grain size coarsening indicates that large grains grow faster than what is assumed in classical normal grain growth theory. We discuss the implications of this model for a mineral that can be deformed under both dislocation creep and grain size sensitive diffusion creep using experimental data of olivine. Our predictions of the piezometric equilibrium in the dislocation-creep regime are in very good agreement with the observations for this major mantle-forming mineral. We show that grain size reduction occurs even when the average grain size is in diffusion creep, because the largest grains of the grain size distribution can still undergo recrystallization. The resulting rheology that we predict for olivine is time-dependent and more non-linear than in dislocation creep. As the deformation rate remains an increasing function of the deviatoric stress, this rheology is not localizing.

Key words: Plasticity, diffusion and creep; Creep and deformation; Fault zone rheology; Dynamics of lithosphere and mantle; High strain deformation zones; Rheology, crust and lithosphere.

GJI Mineral physics, rheology, heat flow and volcanology

1 INTRODUCTION

The localization of deformation in narrow shear bands is necessary for plate tectonics to occur (see e.g. Bercovici *et al.* 2000). Weak faults can be formed during deformation but their weakness can persist even after a reorganization of the large scale stress pattern (e.g. Gurnis *et al.* 2000). This indicates that the rheology is not only controlled by the instantaneous stress field but has memory and healing.

Localization occurs by a feed-back between the rheological law and the deformation wherein a faster deformation can be obtained with a lower stress. In simple shear experiments, this happens when the derivative of deviatoric stress τ with respect to strain-rate $\dot{\epsilon}$ is negative (Bercovici 1993; Montési & Zuber 2002). The fact that the rheology of silicates is often expressed by a non-linear expression with $\epsilon \propto \tau^n$ and $n \geq 1$ (Ranalli 1995) does not lead to strike slip localization as τ remains a monotonically increasing function of $\dot{\epsilon}$ (Bercovici 1995). Non-linear rheologies with large positive exponents tend, however, to narrow the zones of deformation (Weinstein & Olson 1992; Landuyt & Bercovici 2009).

Shear heating has often been proposed as a source of localization that provides some long term memory to the rheology (the thermal diffusion time) (Fleitout & Froidevaux 1980; Leloup *et al.* 1999; Kameyama *et al.* 1997). Unfortunately, although shear heating is necessarily associated with localization, it does not seem to explain either the narrowness of plate boundaries, or their geometries (e.g. Bercovici & Karato 2003). A local increase of porosity/microcracks occurring during deformation has also been invoked for localizing the deformation (Bercovici 1998; Ogawa 2003) but this process is not efficient in 3-D simulations at generating toroidal motions, for example, shearing between plates and plate rotations (Bercovici & Ricard 2005). Anisotropic mechanical behaviour due to an inherited preferred orientation of crystals could also control or favour the localization (e.g. Bystricky *et al.* 2000; Tommasi *et al.* 2009). Once the localization is effective, minor mineralogical phases like serpentine can also lubricate the motion (Hilairet *et al.* 2007).

Grain size reduction seems the most attractive physical process for explaining the initial localization of the deformation. Cataclastic fracturing and recrystallization are well known mechanisms of grain

size reduction and the ductile deformation in the diffusive regime is facilitated in the presence of small grains (Kelemen & Hirth 2007). However, models of localization by grain size reduction are not self-consistent. Recrystallization is observed in the dislocation regime (i.e. when the microscopic deformation proceeds by coherent motion of crystal dislocations rather than by the individual diffusion of atoms and vacancies). Grain size reduction and localization by grain size sensitive rheology occur therefore in somewhat exclusive regimes (Karato *et al.* 1980; Derby & Ashby 1987). Various models have however discussed the possible interactions between large scale deformation and grain size evolution (Kameyama *et al.* 1997; Braun *et al.* 1999; Montési & Hirth 2003; Bercovici & Ricard 2005).

Up to now, most attempts to model the evolution of grain sizes have been derived from phenomenologic laws involving only a mean grain size. A few attempts have been made to describe in a very general way the evolution of an assemblage of grains under deformation (e.g. Slotemaker 2006; Ricard & Bercovici 2009). In these approaches, one has to consider the complete distribution of grains $\nu(\mathcal{R}, \mathbf{X}, t)$ (which is the number of grains per unit volume near the position $\mathbf{X}$ and at time t, having a size between $\mathcal{R}$ and $\mathcal{R} + d\mathcal{R}$). Although a general and physically consistent theory has been proposed (Ricard & Bercovici 2009), the mathematical formalism remains cumbersome and a general implementation in a 3-D and time dependent geodynamic simulation seems implausible.

The approach followed by Ricard & Bercovici (2009) shows that the grain size reduction cannot be related to the stress or to the strain-rate tensor, alone, but necessarily to their scalar product $\underline{\boldsymbol{\tau}} : \underline{\dot{\boldsymbol{\epsilon}}}$ (where $\underline{\boldsymbol{\tau}} : \underline{\dot{\boldsymbol{\epsilon}}} = \Sigma_{ij} \tau_{ij} \dot{\epsilon}_{ij}$). This result is based on the second law of thermodynamics that requires the positivity of the entropy sources. This theoretical requirement already used in Bercovici & Ricard (2005), has been confirmed empirically by Austin & Evans (2007) that concluded that the grain size is a 'paleowattmeter' (i.e. a measure of the rate of dissipation) rather than a 'paleo piezometer' (i.e. a measure of the deviatoric stress).

At a microscopic level and laboratory scale there are a large number of observations regarding the evolution of silicate rheology with grain size, pressure, temperature and stress (but also, water content, oxygen fugacity, porosity...). At the same time, models of mantle convection simulate the existence of plates with ad hoc rheologies (Tackley 2000; Stein *et al.* 2004). Up to now, these models are not based on experiments but often assume that the lithosphere has a linear viscosity with a plasticity threshold. The goal of this paper is to provide a theory based on laboratory experiments that could be used in large scale geodynamic modelling.

2 EVOLUTION OF GRAIN SIZE DISTRIBUTION

Within a volume of material, there is a continuous distribution of grain sizes, $\nu(\mathcal{R}, \mathbf{X}, t)$, so that the number of grains dn with sizes between $\mathcal{R}$ and $\mathcal{R} + d\mathcal{R}$, per unit volume dV, at position $\mathbf{X}$ and time t is

$$dn(\mathcal{R}, \mathbf{X}, t) = \nu(\mathcal{R}, \mathbf{X}, t) \, d\mathcal{R} \, dV. \qquad (1)$$

The distribution ν has units of m^{-4}. From this distribution, average quantities like the mean grain size can be computed. The equations for grain size evolution that have been proposed are empirical and consider the mean grain size only. Here, we also derive an equation for the mean grain size but from theoretical thermodynamic considerations, starting explicitly from the existence of the grain size distribution.

The grain size distribution evolves through two different processes. First, mass transfer between grains can occur continuously through grain boundary migration or diffusion. This involves a change in the number of grains dn in the bin of size $\mathcal{R}$ (i.e. a change in the number of grains of sizes between $\mathcal{R}$ and $\mathcal{R} + d\mathcal{R}$) by coarsening of smaller grains (or continuous reduction of larger grains). This can be described by introducing the rate of movement of the grain in size space $\dot{\mathcal{R}} = \partial \mathcal{R}(\mathbf{X}, t)/\partial t$ (Lifshitz & Slyozov 1961). Mathematically, this process occurs at constant total number of grains per unit volume (experimentally, smallest grains shrink below observability). Second, the number of grains of a given size can be populated by a discontinuous transfer from remote population bins. For example, large grains can be subdivided by the formation of sub-grain boundaries that nucleate new small grains (Hobbs 1968), or can be broken by cataclasis. We call $\Gamma(\mathcal{R})$ the rate at which grains are added to or removed from the bin of size $\mathcal{R}$ by discontinuous process. This discontinuous process changes the total number of grains per unit volume. The balance of grain population implies a continuity equation for the grain size distribution itself (Hillert 1965; Atkinson 1988; Ricard & Bercovici 2009)

$$\frac{\partial \nu}{\partial t} + \frac{\partial \dot{\mathcal{R}} \nu}{\partial \mathcal{R}} = \Gamma, \qquad (2)$$

where t is time. For simplicity we omit the space variable $\mathbf{X}$ and the advection term $\nabla \cdot (\mathbf{v} \nu)$ where $\mathbf{v}(\mathbf{X}, t)$ is the macroscopic velocity of the grained medium (Ricard & Bercovici 2009).

Most attempts of modelling grain coarsening or damage have assumed that the whole grain size distribution can be obtained by the knowledge of its mean grain size (*cf.* De Bresser *et al.* 2001; Ricard & Bercovici 2009). Representing the whole grain size distribution by only a single size scale (e.g. some average) means mathematically that the distribution is self-similar, that is,

$$\nu(\mathcal{R}, t) = A(\mathcal{R}_0) H(u), \qquad (3)$$

where $\mathcal{R}_0$ is some average grain size function of t that will be defined later, $u = \mathcal{R}/\mathcal{R}_0$ is the self-similarity variable and A is an amplitude. This self-similarity assumption is supported experimentally (e.g. Slotemaker 2006) although exceptions exist such as abnormal grain growth (Hillert 1965). Self-similarity has also a mathematical justification. If one solves the eq. (2) starting from any arbitrary distribution and for quite general assumptions for $\dot{\mathcal{R}}$ or Γ, the distribution evolves toward a self-similar solution like (3), after sufficiently long time. This mathematical result has been used in various classical studies of grain coarsening (Lifshitz & Slyozov 1961; Wagner 1961; Hillert 1965), grain fragmentation or aggregation (Collet 2004) and is valid under more general assumptions (Ricard & Bercovici 2009). Our basic start is therefore that although the self-similarity may not be strictly valid, the system remains close enough to a self-similar state than a mean size theory remains useful and is a reasonable compromise between the complexity of a general grain size distribution theory and what can be constrained by the available observations. Future observations of time evolution of grain size variance, skewness and other higher moments of the grain size distribution will be needed to adjust the parameters of a more general theory.

The mass conservation equation, assuming a constant density of grains, implies that the unit volume is just the sum of the volumes of grains, which leads to the normalization

$$\int_0^\infty \check{\mathbf{v}} \nu(\mathcal{R}) \, d\mathcal{R} = 1, \qquad (4)$$

where

$$\check{\mathbf{v}} = \frac{4}{3}\pi \mathcal{R}^3 \tag{5}$$

is the grain volume. The notations follow Ricard & Bercovici (2009) and the breve accent (e.g. ˘) represents variables at the grain size level. The grains are assumed to be spherical, but more complex shapes could be handled easily by replacing π by a comparable factor accounting for polyhedral grain shapes (see Ricard & Bercovici 2009). In the normalization (4), we omit the space and time variables and we integrate the distribution over all grain sizes, potentially from $\mathcal{R} = 0$ to $\mathcal{R} = +\infty$ (we assume that H is zero after some finite value or is well-behaved enough that all the integrals containing H converge at $u = +\infty$).

Using the self similar expression (3), this normalization condition implies

$$A(\mathcal{R}_0) = \frac{3}{4\pi\lambda_3}\frac{1}{\mathcal{R}_0^4} \tag{6}$$

where we define, as in Ricard & Bercovici (2009),

$$\lambda_n = \int_0^\infty u^n H(u)\,du. \tag{7}$$

The amplitude $A(\mathcal{R}_0)$ is therefore related to the grain size distribution H.

3 AVERAGE GRAIN COARSENING AND DAMAGE

The rules of differentiation applied to distribution (3) taking into account the time dependence of the amplitude (6) lead to

$$\frac{\partial v}{\partial t} = -\frac{3}{4\pi\lambda_3}\frac{1}{R_0^5}\frac{d\mathcal{R}_0}{dt}\frac{1}{u^3}\frac{\partial u^4 H}{\partial u}. \tag{8}$$

This proves that $\partial v/\partial t$ is also a self similar function as it can be written as a function of $\mathcal{R}_0$ times a function of u. As $\partial v/\partial t$ appears in the evolution eq. (2), $\partial \dot{\mathcal{R}}v/\partial \mathcal{R}$ (and therefore $\dot{\mathcal{R}}$) and Γ must also be self similar (or have non self similar contributions that cancel each other and are irrelevant to the grain size evolution). Γ is therefore the product of a time-dependent (or $\mathcal{R}_0$-dependent) amplitude $C(\mathcal{R}_0)$ times a shape functions of $u = \mathcal{R}/\mathcal{R}_0$ such that

$$\Gamma = \frac{3}{4\pi\lambda_3\mathcal{R}_0^5}C(\mathcal{R}_0)\frac{1}{u^3}\frac{\partial u^4 H}{\partial u}, \tag{9}$$

(the coefficient $3/(4\pi\lambda_3\mathcal{R}_0^5)$ is included for subsequent simplification). Similarly, given (2) and (8), $\dot{\mathcal{R}}$ can be written as

$$\dot{\mathcal{R}} = B(\mathcal{R}_0)\frac{1}{H}\left(b + \int_0^u \frac{1}{v^3}\frac{\partial v^4 H}{\partial v}dv\right)$$
$$= B(\mathcal{R}_0)\left(\frac{b}{H} + u + \frac{3}{H}\int_0^u Hdv\right) \tag{10}$$

and where $B(\mathcal{R}_0)$ is an amplitude factor. The integration constant b can be obtained from the condition of mass conservation (see Ricard & Bercovici 2009)

$$\int_0^\infty \check{\mathbf{v}}\Gamma(\mathcal{R})d\mathcal{R} = 0 \text{ and } \int_0^\infty \frac{d\check{\mathbf{v}}}{dt}v(\mathcal{R})d\mathcal{R} = 0, \tag{11}$$

where $\check{\mathbf{v}}$ is the volume of a grain (5). This assumes that mass is conserved either during the fusion or fission of grains (first equality) or during continuous mass transfer between grains (second equality).

According to (3), (9) and (15), these two equations become

$$\int_0^\infty \frac{du^4 H}{du}du = 0 \text{ and } \int_0^\infty u^2(b + uH + 3\int_0^u H\,dv)du = 0. \tag{12}$$

The first condition is already verified provided that $u^4 H$ is zero for $u = 0$ and $u = +\infty$. Then, by using an integration by parts,

$$\int_0^X \left(3u^2 \int_0^u Hdv\right)du = \left[u^3 \int H\,du\right]_0^X - \int_0^X u^3 H\,du \tag{13}$$

in the limit of $X \to +\infty$, we therefore prove that mass conservation implies

$$b = -3\int_0^{+\infty} H\,du. \tag{14}$$

which allows us to write

$$\dot{\mathcal{R}} = B(\mathcal{R}_0)\left(u - \frac{3}{H}\int_u^{+\infty} Hdv\right). \tag{15}$$

As the u-shapes of Γ and $\dot{\mathcal{R}}$ are derived from (2), which is itself another expression of the condition of mass conservation, it is not surprising that mass conservation is naturally satisfied.

When the self similar expressions (9) and (15) are introduced back into (2), the shape function can be eliminated and only a differential equation for the average size $\mathcal{R}_0$ remains

$$\frac{d\mathcal{R}_0}{dt} = B(\mathcal{R}_0) - C(\mathcal{R}_0). \tag{16}$$

Up to now the signs of $B(\mathcal{R}_0)$ and $C(\mathcal{R}_0)$ are not known. The goal is therefore to constrain these quantities which control the kinetics of continuous and discontinuous grain processes, respectively from observations guided by the necessary condition of positivity of entropy production.

4 ENERGY CONSIDERATIONS

During deformation, part of the input energy is simply dissipated (entropy) and part is stored reversibly (work). The irreversible energy is dissipated as heat although some minor entropy component (here neglected) can be associated with interfaces when the surface energy is temperature dependent (Bailyn 1994; Bercovici *et al.* 2001a). Three reversible terms can be considered: the macroscopic elastic energy, the energy of dislocations (Karato 2008) and the surface energy of grains, γ (in J m^{-2}). The elastic energy stored around dislocations is always negligible compared to the surface energy of grains (see Shimizu 2008). When a material is deformed, some of the input energy is initially stored elastically, then some is used to increase the density of dislocations (see, Kohlstedt & Weathers 1980; Karato & Jung 2003). At a given point, the dislocations will rearrange to form subgrain boundaries and later, grain boundaries. The elastic energy around dislocations is therefore mostly a temporary buffer converting some of the deformational work into surface energy. Our assumption is that, in the long term, the energy balance is between the deformational work, the viscous dissipation and the change of grain surfaces. Understanding the grain size evolution is therefore understanding how the macroscopic energy partitions between dissipation (through heat production) and storage (by creation of new grain surface through a temporary elastic stage).

Ricard & Bercovici (2009) show that the energy conservation and the requirement of entropy positivity lead to

$$\int_0^\infty \left(-\frac{2\gamma}{\mathcal{R}}\frac{d\check{\mathbf{v}}}{dt}v(\mathcal{R}) - \frac{3}{2}\frac{2\gamma}{\mathcal{R}}\check{\mathbf{v}}\Gamma(\mathcal{R}) + \underline{\underline{\tau}}:\dot{\underline{\underline{\epsilon}}}\,\check{\mathbf{v}}v(\mathcal{R})\right)d\mathcal{R} \geq 0. \tag{17}$$

Although complex, the meaning of this equation is straightforward. The first term represents the continuous change of surface energy of grains and the second term the surface energy stored or removed by the fusion or fission of grains. The third term represents the energy deposited in each grain by the deformation ($\check{\underline{\tau}}$ and $\check{\underline{\dot{\epsilon}}}$ are the stress and strain-rate in each grain). We retain the term $2\gamma/\mathcal{R}$ as it appears in the Laplace expression for the excess pressure in a sphere due to surface tension γ (γ can either be interpreted as a surface energy (in J m^{-2}) or as the surface tension (in N m^{-1}) (see Bailyn 1994).

The likely most common case of grain size evolution is when the grain growth is dominated exclusively by the diffusive mass exchange in keeping with Lifshitz & Slyozov (1961), Wagner (1961), Feltham (1957), but where grain reduction is driven by the deformation populating the material with small grains issued from 'breaking' large grains. This suggests we look for mechanisms that independently obey to

$$\int_0^\infty -\frac{2\gamma}{\mathcal{R}}\frac{d\check{\mathbf{v}}}{dt}\nu(\mathcal{R})\,d\mathcal{R} \geq 0 \tag{18}$$

and

$$\int_0^\infty \left(-\frac{3}{2}\frac{2\gamma}{\mathcal{R}}\check{\mathbf{v}}\Gamma(\mathcal{R}) + \underline{\tau}:\check{\underline{\dot{\epsilon}}}\check{\mathbf{v}}\nu(\mathcal{R})\right)d\mathcal{R} \geq 0. \tag{19}$$

According to (3), (9) and (15) these two conditions can be readily expressed. The first one, (18), just implies

$$-B(\mathcal{R}_0)\int_0^\infty u\left(uH - 3\int_u^{+\infty}H\,dv\right)du = \frac{1}{2}B(\mathcal{R}_0)\lambda_2 \geq 0, \tag{20}$$

where the equality is obtained by integration by parts (similar to (13) with $n=2$) and where λ_2 is the positive integral defined in (7). This inequality means that $B(\mathcal{R}_0) \geq 0$ and therefore that continuous transport must always lead to grain coarsening. The second inequality imposed by the positivity of entropy sources (19), becomes

$$\frac{3\gamma}{\mathcal{R}_0^2}\frac{\lambda_2}{\lambda_3}C(\mathcal{R}_0) \leq \int_0^\infty \underline{\tau}:\check{\underline{\dot{\epsilon}}}\nu(\mathcal{R})\,d\mathcal{R}. \tag{21}$$

Note that while the continuous coarsening of grains is necessarily an entropy source (i.e. $B(R_0)$ must be positive), the processes of fragmentation/coagulation of grains can be either a source (when $C(R_0) \leq 0$) or a sink (when $C(R_0) \geq 0$) of entropy. The dissipation term itself $\underline{\tau}:\underline{\dot{\epsilon}}$ is always positive.

The process reducing the grain size is an entropy sink $C(R_0) \geq 0$. This term is bounded by the mechanical dissipation expressed by the previous inequality. As advocated in a series of papers (Bercovici *et al.* 2001a,b; Bercovici & Ricard 2005; Ricard & Bercovici 2009), a reasonable and pragmatic choice is to introduce a partitioning function $\check{f}(\mathcal{R},\tau)$, with $0 \leq \check{f}(\mathcal{R},\tau) \leq 1$ so that

$$C(\mathcal{R}_0) = \frac{\mathcal{R}_0^2}{3\gamma}\frac{\lambda_3}{\lambda_2}\int_0^\infty \check{f}\,\underline{\tau}:\check{\underline{\dot{\epsilon}}}\check{\mathbf{v}}\nu(\mathcal{R})\,d\mathcal{R}. \tag{22}$$

The general expression of the grain size evolution (16) becomes therefore

$$\frac{d\mathcal{R}_0}{dt} = B(\mathcal{R}_0) - \frac{\mathcal{R}_0^2}{3\gamma}\frac{\lambda_3}{\lambda_2}\int_0^\infty \check{f}\,\underline{\tau}:\check{\underline{\dot{\epsilon}}}\check{\mathbf{v}}\nu(\mathcal{R})\,d\mathcal{R}. \tag{23}$$

The coarsening term is often given on the form $B(\mathcal{R}_0) = G/\mathcal{R}_0^{p-1}$ (Hillert 1965; Atkinson 1988; Karato 2008) where p is of order 2 (corresponding to a coarsening law where $\mathcal{R}_0 \propto t^{1/2}$). The kinetic term G is temperature dependent, $G = k_0\exp(-E_g/(RT))$ but we

Table 1. Chosen sets of parameters: ([1] from Duyster & Stockhert (2001), [2] from Hirth & Kohlstedt (2003), [3] from Kameyama *et al.* (1997).

Reference case			
Parameter	Value	Unit	
γ	1	J m^{-2}	Surface tension[1]
E_1	530	kJ mol^{-1}	Act. Energy (disl.)[2]
A_1	1.1 10^5	MPa^{-n} s^{-1}	Prefactor[2]
V_1	2 10^{-5}	J mol^{-1} Pa^{-1}	Act. volume[2]
n	3.5		disl. exponent [2]
E_2	375	kJ mol^{-1}	Act. Energy (diff.)[2]
A_2	1.5 10^9	μm^m MPa^{-1} s^{-1}	Prefactor[2]
V_2	5 10^{-6}	J mol^{-1} Pa^{-1}	Act. volume[2]
m	3		diff. exponent[2]
E_g	200	kJ mol^{-1}	Act. Energy (growth)[3]
k_0	2.0 10^4	μm^p s^{-1}	Kinetic factor[3]
p	2		growth exponent[3]

are not aware of an experimentally observed dependence on stress (*cf.* Table 1). We therefore use

$$\frac{d\mathcal{R}_0}{dt} = \frac{G}{p\mathcal{R}_0^{p-1}} - \frac{\mathcal{R}_0^2}{3\gamma}\frac{\lambda_3}{\lambda_2}\int_0^\infty \check{f}\,\underline{\tau}:\check{\underline{\dot{\epsilon}}}\check{\mathbf{v}}\nu(\mathcal{R})\,d\mathcal{R}. \tag{24}$$

5 THE CASE OF LOGNORMAL DISTRIBUTIONS

5.1 Experimental distributions

Various experimental studies have indicated that the grain size distribution is lognormal (e.g. Feltham 1957; Faul & Scott 2006; Slotemaker 2006). The distribution of grain sizes (1) is in this case, a Gaussian when plotted as a function of $\ln\mathcal{R}$, that is,

$$\begin{aligned}dn &\propto \exp\left(-\frac{(\ln(\mathcal{R}/\mathcal{R}_0)^2}{2\sigma^2}\right)d\ln\mathcal{R}\,dV \\ &= \frac{1}{\mathcal{R}}\exp\left(-\frac{(\ln(\mathcal{R}/\mathcal{R}_0)^2}{2\sigma^2}\right)d\mathcal{R}\,dV.\end{aligned} \tag{25}$$

In this expression, σ is the dimensionless variance of the distribution of $\ln(\mathcal{R}/\mathcal{R}_0)$ and $\mathcal{R}_0$ is the 'mean' grain size.

The lognormality of observed grain size distributions is only approximate. In a recent compilation of quartz grain sizes, Stipp *et al.* (2010) argue that the distribution is not lognormal but shows modes indicative of the various processes occurring during dynamic recrystallization. However, to first-order, the distribution observed by Stipp *et al.* (2010) is, in fact, not far from lognormal when plotted in appropriate logarithmic coordinates. We therefore introduce the lognormal shape function

$$H(u) = \frac{1}{\sqrt{2\pi}\sigma u}\exp\left(-\frac{(\ln u)^2}{2\sigma^2}\right), \tag{26}$$

(while experimentalists often use the common (base 10) logarithm, we use the natural logarithm which makes the computations of derivatives and integrals less confusing).

In the following of the paper, we refer to $\mathcal{R}_0$ as a mean grain size, in agreement with experimental literature. However the real mean grain size is defined as

$$\langle\mathcal{R}\rangle = \int_0^\infty \mathcal{R}\nu(\mathcal{R})\,d\mathcal{R}\Big/\int_0^\infty \nu(\mathcal{R})\,d\mathcal{R} = \mathcal{R}_0\exp\left(\frac{\sigma^2}{2}\right) \tag{27}$$

while the true definition of $\mathcal{R}_0$ is $\exp(\langle \ln \mathcal{R} \rangle)$ as using (3),

$$\langle \ln(\mathcal{R}) \rangle = \int_0^\infty \ln(\mathcal{R}) \nu(\mathcal{R}) \, d\mathcal{R} \Big/ \int_0^\infty \nu(\mathcal{R}) \, d\mathcal{R} = \ln(\mathcal{R}_0). \quad (28)$$

The 'mean' grain size reported in most publications is indeed the mean of the grain size distribution plotted as a function of $\ln \mathcal{R}$ rather than $\langle \mathcal{R} \rangle$. The difference between $\mathcal{R}_0$ and $\langle \mathcal{R} \rangle$ decreases with the decreasing variance of the distribution σ, see (27). For a monodisperse distribution of grain sizes (a Dirac distribution) the two quantities become identical. The choice of a lognormal distribution allows us to compute explicitly the integrals that appear in various equations (e.g. 27 or 28). A similar exercise could have been done with any other distribution.

The lognormal distribution means that when the maximum of the grain size distribution is at $\mathcal{R}_0$, the grains of sizes

$$\mathcal{R}_\sigma = \mathcal{R}_0 \exp(\pm \sigma \sqrt{2 \ln 2}) \quad (29)$$

are two times less frequent. From observations on olivine (Slotemaker 2006; Karato 2008), σ seems to be between 0.5 and 1. This indicates that grains, 3 times larger or 3 times smaller than the average grain size are half less probable than grains of the grain size (this estimate uses $\sigma = 0.93$). In other words, the centre of the distribution covers already about one order of magnitude in sizes (3^2) and the tails of the distribution cover another order of magnitude.

With this choice of distribution law, we get

$$\int u^n H(u) \, du = -\frac{1}{2} \exp\left(\frac{n^2 \sigma^2}{2}\right) \mathrm{erf}\left(\frac{n\sigma^2 - \ln(u)}{\sqrt{2}\sigma}\right), \quad (30)$$
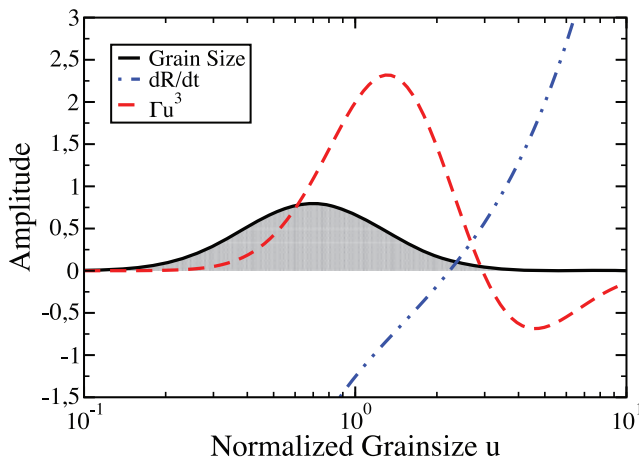
which implies

$$\lambda_n = \int_0^\infty u^n H(u) \, du = \exp\left(\frac{n^2 \sigma^2}{2}\right), \quad (31)$$

$$\dot{\mathcal{R}} = B(\mathcal{R}_0)\left[u - \frac{3}{2H(u)} \mathrm{erfc}\left(\frac{\ln u}{\sqrt{2}\sigma}\right)\right], \quad (32)$$

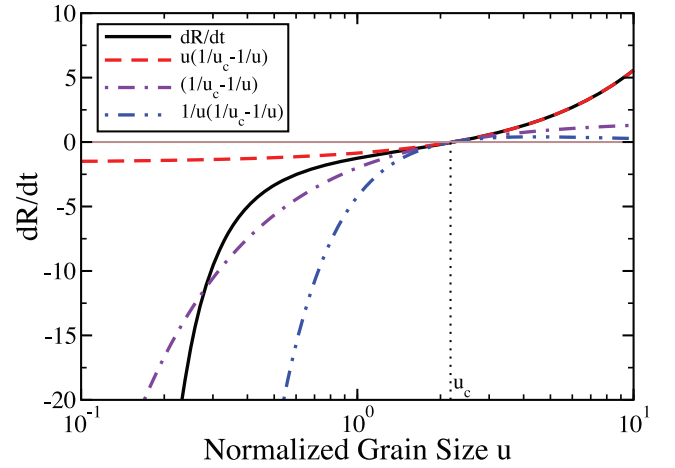where erfc is the complementary error function, $(1 - \mathrm{erf})$ and finally,

$$\Gamma = \frac{3C(\mathcal{R}_0)}{4\pi \lambda_3 \mathcal{R}_0^5} H(u) \left(3 - \frac{\ln u}{\sigma^2}\right). \quad (33)$$

These distributions are plotted in Fig. 1. The function H is shaded and the $\dot{\mathcal{R}}$ and Γu^3 normalized functions (i.e. $\dot{\mathcal{R}}/B(\mathcal{R}_0)$ and $4\pi \lambda_3 \mathcal{R}_0^5 \Gamma u^3/(3C(\mathcal{R}_0))$) are depicted in blue dot-dashed and

Figure 2. The shape of the function $\dot{\mathcal{R}}$, similar to Fig. 1 but with a different scale, is depicted with a black line. Previous studies have assumed that $\dot{\mathcal{R}}$ was given by the red (dashed) (Ricard & Bercovici 2009), purple (dot-dashed) (Hillert 1965) or blue (double-dot-dashed) (Lifshitz & Slyozov 1961) lines. We arbitrary choose the amplitudes of these three later curves so they change sign with the same slopes.

red dashed. We display a curve proportional to Γu^3 instead of Γ to emphasize the negative lobe of the damage term. These two curves change sign roughly at the average grain size around $u = 3$. As expected the function Γ, accounting for the discontinuous formation of grains, implies the breaking of large grains ($\Gamma < 0$ for large $\mathcal{R}$) and thus the formation of small grains ($\Gamma > 0$ for large $\mathcal{R}$). Although the $\dot{\mathcal{R}}$ function (32) seems very complex, it is a simple monotonically increasing function.

Notice that Feltham (1957) in a well-known paper, using an approach that is, in principle, equivalent, writes that a lognormal distribution corresponds approximatively to $\dot{\mathcal{R}} = C'(\mathcal{R}_0) \ln u/u$. His result is not in agreement with our findings. In his demonstration, Feltham (1957) identifies wrongly the grain size distribution with the size distribution of grain sections. The probability to have a grain section of radius r is actually the convolution of the grain size distribution by the probability to cut any grain of radius larger than r, at the specific grain size section of radius r.

The grain growth law, $\dot{\mathcal{R}}$, is not much different from the functions previously used (see Fig. 2), which are based on the inference that the kinetics of intergranular exchange is related to $2\gamma/\overline{\mathcal{R}} - 2\gamma/\mathcal{R} = 2\gamma/\mathcal{R}_0(1/\overline{u} - 1/u)$, that is, the difference between the pressure in a given grain due to its surface tension, $\propto 2\gamma/\mathcal{R}$ and some average grain pressure written as $\propto 2\gamma/\overline{\mathcal{R}}$ (where $\overline{\mathcal{R}}$ is related to the grain size distribution through mass conservation, see 11). When u is large the shape of $\dot{\mathcal{R}}$ looks like $u(1/\overline{u} - 1/u)$, while the shape used by Lifshitz & Slyozov (1961) was $1/u(1/\overline{u} - 1/u)$ and the shape used by Hillert (1965) was $(1/\overline{u} - 1/u)$ (see Fig. 2). The stronger dependence of $\dot{\mathcal{R}}$ with $\mathcal{R}$ at large grain size, suggests that grains significantly larger than the average grain size are more favourable than expected by Lifshitz & Slyozov (1961) or Hillert (1965). These other authors' assumptions yield narrow grain size distributions of finite extent (see Ricard & Bercovici 2009) where the maximum grain size is only twice the average grain size, while observations show distributions with much longer tails (Faul & Scott 2006).

5.2 Microscopic rheology

At grain size level, and for mantle conditions, the olivine rheology is generally found as a mixture of diffusion and dislocation

Figure 1. The lognormal distribution H is shaded. The normalized function Γu^3 is depicted with a red dashed line, the normalized grain growth $\dot{\mathcal{R}}$ by a blue dot-dashed line. The value $\sigma = 0.6$ has been used.

creep (Karato 2008; Hirth & Kohlstedt 1995a,b; Ranalli 1995). At very high stress regimes, other deformation mechanisms might be present like grain boundary sliding (Kohlstedt & Wang 2001; Hirth & Kohlstedt 2003; Drury 2005; Langdon 2006; Kohlstedt 2007) or Peierls mechanisms (Evans & Goetze 1979; Frost & Ashby 1982; Raterron *et al.* 2004; Katayama & Karato 2008; Kohlstedt 2007). We only consider diffusion and dislocation creep laws for simplifications, but other mechanisms could be added. We use

$$\dot{\underline{\varepsilon}} = (a\check{\tau}^{n-1} + b\mathcal{R}^{-m})\underline{\check{\tau}} \tag{34}$$

assuming that the mechanisms of deformation occur in parallel (and $\check{\tau}$ is the second invariant of $\underline{\check{\tau}}$). In (34), the two terms correspond to the dislocation stress-dependent mechanism and to the diffusion grain size-dependent mechanism. Typically $n \sim 3$ and $m \sim 3$ (Hirth & Kohlstedt 2003; Kohlstedt 2007).

The macroscopic rheology $\tau = 2\eta\dot{\epsilon}$ is obtained by computing the volume average deformation rate and stress (see Ricard & Bercovici 2009, for more details). This can be done numerically but not analytically in the more general case although some variational estimates might be possible as in Hashin & Shtrikman (1963). As a simple case, we assume that the stress tensor at the grain size level $\underline{\check{\tau}}$ is uniform and therefore equal to the macroscopic stress $\underline{\tau}$. This is akin to the Reuss averaging in elasticity (Reuss 1930). In this case,

$$\dot{\underline{\epsilon}} = \underline{\tau} \int_0^{+\infty} (a\tau^{n-1} + b\mathcal{R}^{-m})\check{\mathbf{v}}\nu(\mathcal{R})\,d\mathcal{R} \tag{35}$$

and the use of a self-similar distribution (3) allows us to express this relation as a function of average grain size $\mathcal{R}_0$ and stress τ.

$$\dot{\underline{\epsilon}} = \left(a\tau^{n-1} + b\frac{\lambda_{3-m}}{\lambda_3}\mathcal{R}_0^{-m}\right)\underline{\tau} = a\tau^{n-1}\left(1 + \left(\frac{\mathcal{R}_c}{\mathcal{R}_0}\right)^m\right)\underline{\tau}, \tag{36}$$

where

$$\mathcal{R}_c = \left(\frac{b}{a}\frac{\lambda_{3-m}}{\lambda_3}\tau^{1-n}\right)^{1/m} \tag{37}$$

is the average grain size at the macroscopic transition between diffusion and dislocation creeps. The macroscopic rheology is thus a function of the mean grain size $\mathcal{R}_0$ and the grain size distribution through λ_{3-m}/λ_3. Note that when the average grain size is $\mathcal{R}_c$, the macroscopic material is exactly at the transition between diffusion and dislocation, the individual grain with the same radius is still largely in the diffusion regime as $\lambda_{3-m}/\lambda_3 \sim 0.1$ according to (31). The experimentalist that works with a sample containing a distribution of grain sizes cannot measure directly the microscopic rheological factor of diffusion creep b, but only get the macroscopic coefficient $b(\lambda_{3-m}/\lambda_3)$. This coefficient together with the rheological factor a of dislocation creep, are both temperature dependent with an Arrhenius form and their own activation energies, that is,

$$a = A_1 \exp\left(-\frac{E_1}{RT}\right) \quad \text{and} \quad b\frac{\lambda_{3-m}}{\lambda_3} = A_2 \exp\left(-\frac{E_2}{RT}\right), \tag{38}$$

where R is the gas constant.

To provide a simpler expression for the grain size evolution than the general expression (24), we need to know the value of the partitioning energy factor $\check{f}$. In the absence of direct observations, we can make two simple guesses:

(i) The simplest case is to assume a constant partitioning $\check{f} = f_0$. The partitioning is the same irrespective of the deformation mechanism itself. In this case the general grain size evolution would obey

$$\frac{d\mathcal{R}_0}{dt} = \frac{G}{p\mathcal{R}_0^{p-1}} - f_0\frac{\mathcal{R}_0^2}{3\gamma}\frac{\lambda_3}{\lambda_2}\underline{\tau} : \dot{\underline{\epsilon}} \tag{39}$$
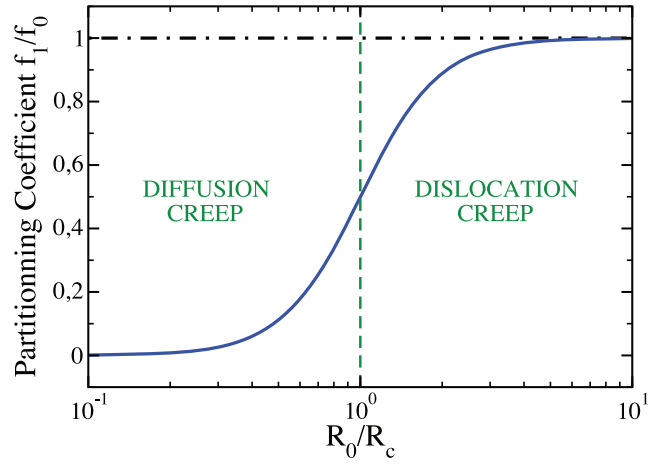
Figure 3. The normalized partitioning function f_1/f_0 (solid blue curve) for a mean grain size varying between 10^{-1} and 10 times the critical grain size at the macroscopic boundary between diffusion and dislocation creep. The transition between diffusion and dislocation creeps occurs through a large range of grain sizes.

(ii) The creation of new grains occurs by formation of subgrain boundaries (Twiss 1977; Derby 1990, 1991; Bresser *et al.* 1998; Shimizu 1998a,b, 1999; Bresser 2002). This requires the presence of dislocations density and it can be argued that the partitioning of energy only occurs during dislocation creep (in each grain, the strain-rate is determined by a mixture of diffusion and dislocation creep, but only the mechanical work done by dislocation creep can be used to form new grains). This means that

$$\frac{d\mathcal{R}_0}{dt} = \frac{G}{p\mathcal{R}_0^{p-1}} - f_0\frac{\mathcal{R}_0^2}{3\gamma}\frac{\lambda_3}{\lambda_2}\underline{\tau} : \dot{\underline{\epsilon}}_{disloc}$$

$$= \frac{G}{p\mathcal{R}_0^{p-1}} - f_1(\tau, \mathcal{R}_0)\frac{\mathcal{R}_0^2}{3\gamma}\frac{\lambda_3}{\lambda_2}\underline{\tau} : \dot{\underline{\epsilon}}, \tag{40}$$

where

$$f_1(\tau, \mathcal{R}_0) = f_0\frac{1}{1 + (\mathcal{R}_c/\mathcal{R}_0)^m}. \tag{41}$$

which is depicted in Fig. 3. The function goes from 0 (no grain reduction occurs when the mean grain is largely in the diffusion regime) to f_0 (all the grains are in the dislocation regime and they all shrink). The partitioning function is independent of σ, the spread of the grain size distribution.

6 APPLICATION TO OLIVINE

The creep map of olivine has been described by various authors (Chopra & Paterson 1981; Karato *et al.* 1986; Karato & Wu 1993; Hirth & Kohlstedt 2003; Korenaga & Karato 2008). We compiled some reference values for exponents, prefactors and activation energies appropriate for dry olivine in Table 1. The exponents n and m are close to $n \simeq 3.5$ and $m \simeq 3$ for dry olivine although Korenaga & Karato (2008) suggest a larger n exponent, $n \simeq 4.94$ for dislocation creep.

There are few studies and more uncertainty for the grain growth kinetics. As a reference case, we use a value of $p = 2$ taken from Karato (1989) and in agreement with the theoretical model of Hillert (1965) and the form of $G = k_0 \exp(-E_g/RT)$ (see Table 1) is identical to that chosen in Kameyama *et al.* (1997). This choice based on Karato (1989) leads to a grain growth much faster than what is obtained in Evans *et al.* (2001) or Faul & Scott (2006) who

use $p = 4.3$ and much larger than what is expected from observations of natural peridotites. Grain boundary pinning by impurities and minor phases may explain this discrepancy.

Eqs (39) and (40) imply the existence of steady state regime, $d\mathcal{R}_0/dt = 0$ where a constant grain size results from balancing grain coarsening by dynamic recrystallization. If we use (40), coarsening can only be driven by energy subtracted from the dissipation associated with dislocations. In this case, the steady state regime usually called piezometric equilibrium (Van der Wal *et al.* 1993; Bresser *et al.* 1998) satisfies

$$\mathcal{R}_0 = \left(\frac{3\gamma}{p} \frac{G}{fa} \right)^{1/(p+1)} \tau^{-(n+1)/(p+1)}. \tag{42}$$

This equilibrium, where $\mathcal{R}_0 \propto \tau^{-1.5}$, occurs both in the dislocation and diffusion regimes because even in the diffusive regime, the larger grains in the grain size distribution are still subject to dynamic recrystallization. If even the energy subtracted from dissipation in the diffusive regime contributes to grain size reduction, as in (39), another equilibrium can be reached with

$$\mathcal{R}_0 = \left(\frac{3\gamma}{p} \frac{G\lambda_2}{fb\lambda_{3-m}} \right)^{1/(p+1-m)} \tau^{-2/(p+1-m)}. \tag{43}$$

In the case $p = 2$ and $m = 3$, as $p + 1 - m = 0$, this equilibrium becomes independent of $\mathcal{R}_0$ and simply defines a plasticity threshold, $\tau_c = (3\gamma G\lambda_2/pfb\lambda_{3-m})^{1/2}$.

Fig. 4, depicts the domains of dislocation dominant and diffusion dominant creeps for olivine at 1923 K. The dot-dashed black and solid blue curves indicate the equilibrium states ($\partial\mathcal{R}_0/\partial t = 0$) predicted by (42) and (43) when we choose $f_0 = 1.5 \, 10^{-6}$ (f_0 controls the intercepts of the theoretical piezometers, not their slopes). All grains below these curves grow until they reach the piezometric curve and reciprocally, above these curves the dynamic recrystallization dominates and the grain size decreases. Purple squares represent experimental data from Karato *et al.* (1980) which fit our model for the chosen f_0. In the diffusion creep domain, no experimental points are available. This is reasonable because if the hypothesis (39) is true, the plasticity threshold forbids any equilibrium in the diffusive regime. Even in the case where the recrystallization
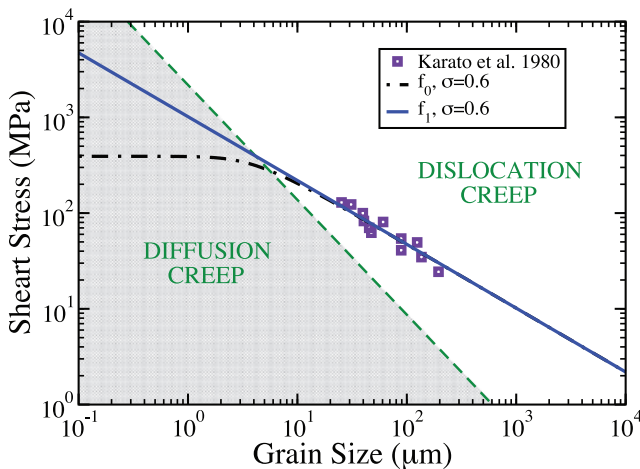
Figure 4. Equilibrium curves using our two approximations. We use the standard set of rheologies displayed in table 1, $T = 1923$ K, $P = 1$ atm. The green shaded area corresponds to the zone where the rheology is predominantly in the diffusive regime. The equilibrium state (or piezometer) in the dislocative regime goes through the experimental points (Karato *et al.* 1980). A plasticity threshold is predicted for the case defined by (39) (label f_0).
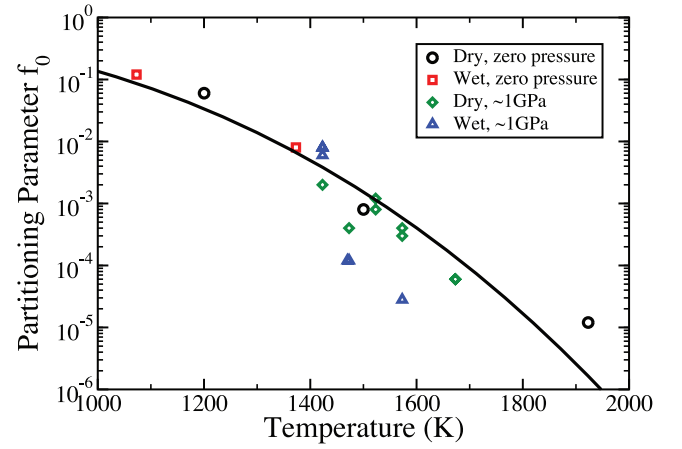
Figure 5. Various experimental piezometers can be fitted by choosing $f_0 = \exp(-2.0\,(T/1000)^{2.9})$. The fit does not seem to depend much on the pressure or the water content.

is only controlled by the dislocation, i.e. using (40) (Fig. 4, blue curve), the equilibrium in the diffusive domain may be difficult to identify. Indeed, as the equilibrium grain size is stress dependent, $\mathcal{R}_0 \propto \tau^{-1.5}$, the diffusive grain size dependent rheology appears, at equilibrium, more stress dependent than in the dislocation domain since $\dot{\epsilon} \propto \mathcal{R}_0^{-3}\tau = \tau^{5.5}$. The experimentalist may interpret the data as an indication of grain boundary sliding rather than diffusion.

Fig. 4 is computed at $T = 1923$ K. Other experimental piezometers have been proposed at different temperature and for olivine with different water contents (Post 1977; Karato *et al.* 1980; Ross *et al.* 1980; Van der Wal *et al.* 1993; Zhang *et al.* 2000; Jung & Karato 2001; Jung *et al.* 2006). For each set of experiments we can obtain an appropriate value for f_0. These different values are depicted in Fig. 5. We also infer an empirical fit $f_0 = \exp(-2.0(T/1000)^{2.9})$ that agrees with the requirement $0 \leq f_0 \leq 1$. The partitioning factor decreases significantly with temperature and does not seem to vary much with pressure or water content (f_0 might decrease slightly with water content and increase slightly with pressure). The non-equilibrium thermodynamics imposes the form of the evolution equation and bounds the possible values of f_0, but at this stage, we have not tried to derive this parameter from a microscopic kinetic model.

When the grain size evolves with time and stress, the rheology becomes itself a time dependent function. We illustrate this point in Fig. 6. We start with an olivine with very small grain size (1 μm) and impose a constant deviatoric stress at a temperature of 1100 K. In this case, the rheology is initially Newtonian, that is, in the diffusion creep (dashed line). However, the grains coarsen or shrink (at very large stress) and the rheology becomes non-linear. For low deviatoric stresses (below 300 MPa), the equilibrium rheology is dislocative (stress exponent 3). For larger stresses, the grains deform under diffusion creep but as the grain size is stress dependent, the equilibrium rheology is also non-linear (stress exponent 5.5).

Another illustration of the time dependence of the rheology is provided in Fig. 7. We compute a stress profile within an oceanic lithosphere with age 50 Myr (the temperature is an error function with standard parameters). A uniform strain-rate $\dot{\epsilon} = 10^{-15}$ s^{-1} is imposed (Goetze & Evans 1979). We assume that the average grain size is initially $\mathcal{R}_0 = 1$ μm and, except in the shallower zone where the stress is limited by Byerlee failure criterion (Byerlee 1978), diffusion creep prevails. The grain size then evolves quite rapidly and the strength of the lithosphere increases with time. The
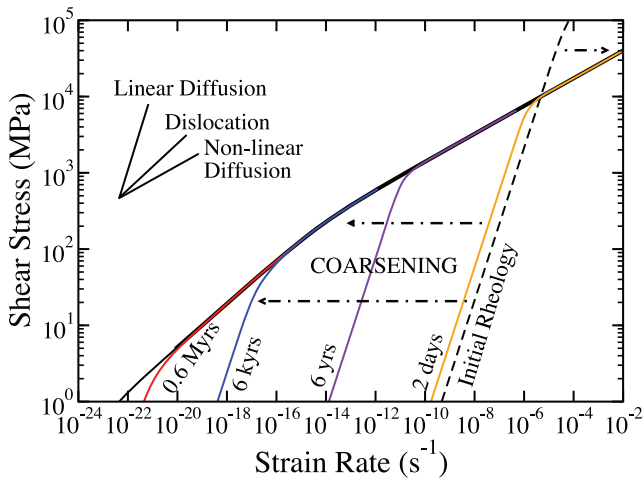
Figure 6. Evolution of the rheology with increasing grain size (from $1 \mu m$). The shear stress varies initially with the strain-rate as τ (diffusive case), then as $\tau^{1/3.5}$ (dislocative case, for $\tau < 300$ MPa), or as $\tau^{1/5.5}$ (diffusive case with stress dependent grain size).

lithosphere recovers in a few 10 kyr. At equilibrium, the lithosphere is in the dislocation regime at large depth (above 50 km). From 20 to 50 km, the presence of small average grain sizes places the rheology in the diffusive regime. In this layer whose deeper limit is marked by a kink in the equilibrium grain size (see Fig. 7, bottom panel), the rheology is in fact more stress-dependent than in the underlying layer undergoing dislocation creep.

7 DISCUSSION AND CONCLUSION

In this paper, we started from simple thermodynamics requirements to derive a very general equation for grain size evolution. Our method takes into account the spread of the grain size distribution and considers that, at a given time and around a given position, not all grains deform with the same creep mechanism. Large grains can be submitted to recrystallization while the small grains can deform then coarsen in the diffusive regime. A corollary of our approach is that the kinetics of coarsening and recrystallization can be estimated from the grain size distribution itself. Experimental observations suggest that the growth of large grains is faster than what was considered in the classic theories of Lifshitz & Slyozov (1961) or Hillert (1965).

We infer a grain size equation of the form

$$\frac{d\mathcal{R}_0}{dt} = \frac{G}{p\mathcal{R}_0^{p-1}} - f_0 \frac{1}{1 + (\mathcal{R}_c/\mathcal{R}_0)^m} \frac{\mathcal{R}_0^2}{3\gamma} \frac{\lambda_3}{\lambda_2} \underline{\tau} : \underline{\dot{\epsilon}}, \tag{44}$$

where $\mathcal{R}_c$ is the transitional grain radius between diffusion and dislocation. This equation assumes the self similarity of the grain sizes within a lognormal distribution. As already stated, self-similarity is approximately verified experimentally and is the consequence of the equation of grain size distribution itself (2) whose solutions tend to self-similarity. If we reject this hypothesis, then we need to derive the expressions for $\dot{\mathcal{R}}$ and Γ directly from observations. The difficulty is then not so much with the mathematics than with the experiments: reporting the evolution of the average grain size but not the evolution of the grain size distribution itself is not sufficient to constrain the kinetics of grain diffusion and recrystallization.

The rheology of the grained material is naturally non-linear and time-dependent (it could also be anisotropic which is another complexity not accounted for in this paper Tommasi *et al.* 2009). This
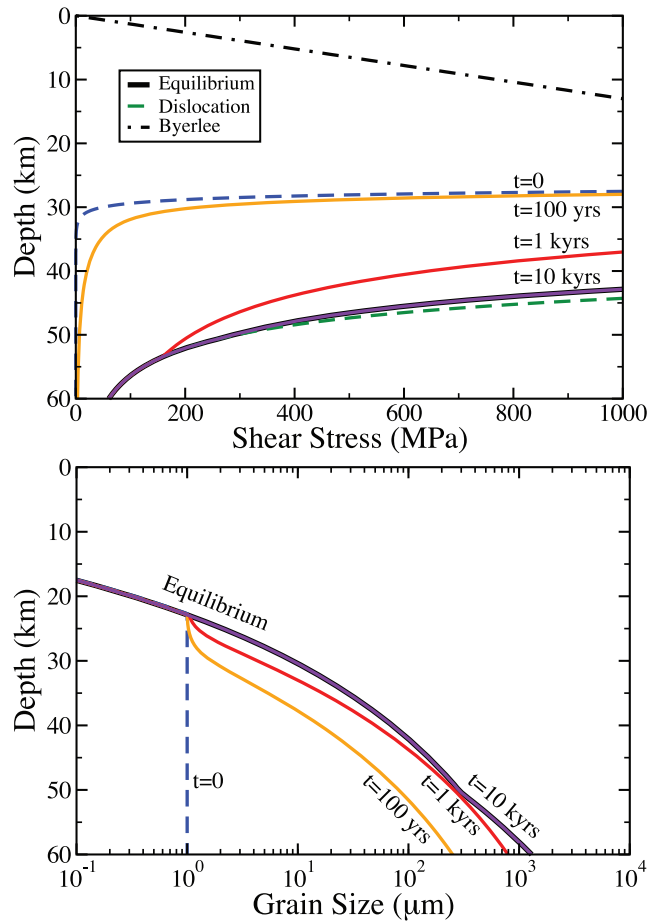
Figure 7. Time dependent stress profile (top) and time dependent grain size profile (bottom). The initial grain size is $d = 1 \mu m$, a constant and uniform strain-rate is assumed, across a 50 Myr oceanic lithosphere.

provides a memory to the mechanical behaviour of the lithosphere, an ingredient that is missing to the models of convection with self-consistent plates (i.e. Tackley 2000; Stein *et al.* 2004). When the grain size-stress relation is taken into account, we predict that the diffusive rheology is more stress-dependent than the dislocative rheology, in contradiction with traditional rheological models.

At equilibrium, the strain-rate remains an increasing function of the stress and the rheology appears to be monotonic and simply non-linear with an exponent varying from 3.5 to 5.5. This is however, a very partial view of the rich dynamics implied by eq. (44). In a realistic time dependent situation, the rheology maybe far from equilibrium and the effective stress–strain-rate relation can be much more complex than at equilibrium. The dynamics is also affected by the feedback between deformation and heat production by viscous dissipation as various parameters are temperature dependent. All these aspects are beyond the scope of the present paper but will be studied in the future.

The eq. (44) can be compared to what is used in various publications (Kameyama *et al.* 1997; Braun *et al.* 1999; Bercovici & Karato 2003).

$$\frac{d\mathcal{R}_0}{dt} = s \frac{G}{p\mathcal{R}_0^{p-1}} - \frac{\dot{\epsilon}}{\dot{\epsilon}_T}(\mathcal{R}_0 - \mathcal{R}_P), \tag{45}$$

where s goes from 1 in the diffusion domain to 0 in the dislocation domain, $\dot{\epsilon}_T$ is an experimental parameter and $\mathcal{R}_P$ the equilibrium grain size function of stress.

Our formalism (44) differs from what has been used previously (45) by various points. We assume that coarsening occurs even in the dislocation regime while (45) considers that it only happens in the diffusion regime (although Bercovici & Karato 2003, use 45 with $s = 1$). Using non-equilibrium thermodynamics, we prove that grain reduction is related to the energy dissipated in the system, not to the strain-rate alone. In our model, the term representing recrystallization always reduces the grain size while in (45), recrystallization facilitates grain coarsening when $\mathcal{R}_0 < \mathcal{R}_P$. At last, we predict the piezometric equilibrium while (45) must include an equilibrium radius $\mathcal{R}_P$ which is not consistently deduced by the model itself.

REFERENCES

Atkinson, H., 1988. Theories of normal grain growth in pure single phase systems, *Acta. Metall.,* **36,** 469–491.

Austin, N.J. & Evans, B., 2007. Paleowattmeters: a scaling relation for dynamically recrystallized grain size, *Geology,* **35,** 343–346.

Bailyn, M., 1994. *A Survey of Thermodynamics,* Am. Inst. Phys., College Park, Md.

Bercovici, D., 1993. A simple model of plate generation from mantle flow, *Geophys. J. Int.,* **114**(3), 635–650.

Bercovici, D., 1995. A source-sink model of the generation of plate tectonics from non-newtonian mantle flow, *J. geophys. Res.,* **100,** 2013–2030.

Bercovici, D., 1998. Generation of plate tectonics from lithosphere-mantle flow and void-volatile self-lubrication, *Earth planet. Sci. Lett.,* **154,** 139–151.

Bercovici, D. & Karato, S., 2003. Theoretical analysis of shear localization in the lithosphere, in *Reviews in Mineralogy and Geochemistry: Plastic Deformation of Minerals and Rocks,* Vol. 51, chap. 13, pp. 387–420, eds Karato, S. & Wenk, H., Min. Soc. Am., Washington, DC.

Bercovici, D. & Ricard, Y., 2005. Tectonic plate generation and two-phase damage: void growth versus grainsize reduction, *J. geophys. Res.,* **110,** B03401, doi:10.1029/2004JB003401.

Bercovici, D., Ricard, Y. & Richards, M., 2000. The relation between mantle dynamics and plate tectonics: a primer, in *History and Dynamics of Global Plate Motions*, Geophys. Monogr. Ser., Vol. 121, pp. 5–46, eds Richards, M.A., Gordon, R. & van der Hilst, R., Am. Geophys. Union, Washington, DC.

Bercovici, D., Ricard, Y. & Schubert, G., 2001a. A two-phase model of compaction and damage, 1. general theory, *J. geophys. Res.,* **106**(B5), 8887–8906.

Bercovici, D., Ricard, Y. & Schubert, G., 2001b. A two-phase model of compaction and damage, 3. applications to shear localization and plate boundary formation, *J. geophys. Res.,* **106**(B5), 8925–8940.

Braun, J., Chery, J., Poliakov, A., Mainprice, D., Vauchez, A., Tomassi, A. & Daignieres, M., 1999. A simple parameterization of strain localization in the ductile regime due to grain size reduction: A case study for olivine, *J. geophys. Res.*, **104,** 25 167–25 181.

Bresser, J.H.P.D., 2002. On the mechanism of dislocation creep of calcite at high temperature: inferences from experimentally measured pressure sensitivity and strain rate sensitivity of flow stress, *J. geophys. Res.*, **107**(B12), doi:10.1029/2002JB001812.

Bresser, J.H.P.D., Peach, C.J., Reijs, J.P.J. & Spiers, C.J., 1998. On dynamic recrystallization during solid state flow: effects of stress and temperature, *Geophys. Res. Lett.,* **25,** 3457–3460.

Byerlee, J.D., 1978. Friction of rocks, *Pure appl. Geophys.,* **116,** 615–626.

Bystricky, M., Kunze, K., Burlini, L. & Burg, J.-P., 2000. High Shear Strain of Olivine Aggregates: rheological and Seismic Consequences, *Science,* **290**(5496), 1564–1567.

Chopra, P.N. & Paterson, M.S., 1981. The experimental deformation of dunite, *Tectonophysics,* **78,** 453–473.

Collet, J.-F., 2004. Some modelling issues in the theory of fragmentation-coagulation systems, *Commun. Math. Sci.,* **2**(Suppl. 1), 35–54.

De Bresser, J.H.P., Heege, J.H.T. & Spiers, C.J., 2001. Grain size reduction by dynamic recrystallization: can it result in major theological weakening?, *Int. J. Earth Sciences,* **90,** 28–45.

Derby, B., 1990. Dynamic recrystallization and grain size, in *Deformation Processes in Minerals, Ceramics and Rocks,* pp. 354–364, eds Barber, D. & Meredith, P., Unwin Hyman, London.

Derby, B., 1991. The dependence of grain size on stress during dynamic recrystallization, *Acta Metall. Mater.,* **39,** 955–962.

Derby, B. & Ashby, M., 1987. On dynamic recrystallization, *Scr. Metall.,* **21,** 879–884.

Drury, M., 2005. Dynamic recrystallization and strain softening of olivine aggregates in the laboratory and the lithosphere, *Geol. Soc., Lond., Spec. Publ.,* **243,** 143–158.

Duyster, J. & Stockhert, B., 2001. Grain boundary energies in olivine derived from natural microstructures, *Contrib. Mineral. Petrol.,* **140,** 567–576.

Evans, B. & Goetze, C., 1979. The temperature variation of the hardness of olivine and its implication for polycrystalline yield stress, *J. geophys. Res.,* **84**(B10), 5505–5524.

Evans, B., Renner, J. & Hirth, G., 2001. A few remarks on the kinetics of static grain growth in rocks, *Int. J. Earth Sci.,* **90,** 88–103.

Faul, U.H. & Scott, D., 2006. Grain growth in partially molten olivine aggregates, *Contrib. Mineral. Petrol.,* **151,** 101–111.

Feltham, P., 1957. Grain growth in metals, *Acta. Metall.,* **5,** 97–105.

Fleitout, L. & Froidevaux, C., 1980. Thermal and mechanical evolution of shear zones, *J. Struct. Geol.,* **2,** 159–164.

Frost, H. & Ashby, M., 1982. *Deformation-Mechanism Maps: The Plasticity and Creep of Metals and Ceramics,* Pergamon Press, Oxford.

Goetze, C. & Evans, B., 1979. Stress and temperature in the bending lithosphere as constrained by experimental rock mechanics, *Geophys. J. R. astr. Soc.,* **59**(3), 463–478.

Gurnis, M., Zhong, S. & Toth, J., 2000. On the competing roles of fault reactivation and brittle failure in generating plate tectonics from mantle convection, in *History and Dynamics of Global Plate Motions*, Geophys. Monogr. Ser., Vol. 121, pp. 73–94, eds Richards, M.A., Gordon, R. & van der Hilst, R., Am. Geophys. Union, Washington, DC.

Hashin, Z. & Shtrikman, S., 1963. A variational approach to the theory of the elastic behaviour of multiphase materials, *J. Mech. Phys. Solids,* **11,** 127–140.

Hilairet, N., Reynard, B., Wang, Y., Daniel, I., Merkel, S., Nishiyama, N. & Petitgirard, S., 2007. High-pressure creep of serpentine, interseismic deformation, and initiation of subduction, *Science,* **318,** 1910–3.

Hillert, M., 1965. On theory of normal and abnormal grain growth, *Acta Metall.,* **13,** 227–230.

Hirth, G. & Kohlstedt, D., 2003. Rheology of the upper mantle and the mantle wedge: a view from the experimentalists, in *Inside the Subduction Factory,* Geophys. Monogr. Ser., Vol. 138, pp. 83–105, ed. Eiler, J., Am. Geophys. Union, Washington, DC.

Hirth, G. & Kohlstedt, D.L., 1995a. Experimental constraints on the dynamics of the partially molten upper mantle: deformation in the diffusion creep regime, *J. geophys. Res.,* **100,** 1981–2001.

Hirth, G. & Kohlstedt, D.L., 1995b. Experimental constraints on the dynamics of the partially molten upper mantle: deformation in the dislocation creep regime, *J. geophys. Res.,* **100,** 15 441–15 449.

Hobbs, B., 1968. Recrystallization of single crystals of quartz, *Tectonophysics,* **6**(5), 353–401.

Jung, H. & Karato, S., 2001. Water-induced fabric transitions in olivine, *Science,* **293**(5534), 1460–1463.

Jung, H., Katayama, I., Jiang, Z., Hiraga, T. & Karato, S., 2006. Effect of water and stress on the lattice-preferred orientation of olivine, *Tectonophysics,* **421,** 1–22.

Kameyama, M., Yuen, D.A. & Fujimoto, H., 1997. The interaction of viscous heating with grain-size dependent rheology in the formation of localized slip zones, *Geophys. Res. Lett.,* **24,** 2523–2526.

Karato, S., 2008. *Deformation of Earth Materials: An Introduction to the Rheology of Solid Earth,* Cambridge University Press, Cambridge.

Karato, S.-I., 1989. Grain growth kinetics in olivine aggregates, *Tectonophysics,* **168,** 255–273.

Karato, S.-I. & Jung, H., 2003. Effects of pressure on high-temperature dislocation creep in olivine, *Phil. Mag.,* **83**(3), 401–414.

Karato, S.I. & Wu, P., 1993. Rheology of the upper mantle: a synthesis, *Science,* **260,** 771–778.

Karato, S.-I., Toriumi, M. & Fujii, T., 1980. Dynamic recrystallization of olivine single crystals during high-temperature creep, *Geophys. Res. Lett.,* **7,** 649–652.

Karato, S.-I., Paterson, M.S. & Fitzgerald, J.D., 1986. Rheology of synthetic olivine aggregates - Influence of grain size and water, *J. geophys. Res.,* **91,** 8151–8176.

Katayama, I. & Karato, S.-I., 2008. Low-temperature, high-stress deformation of olivine under water-saturated conditions, *Phys. Earth planet. Inter.,* pp. 125–133.

Kelemen, P.B. & Hirth, G., 2007. A periodic shear-heating mechanism for intermediate-depth earthquakes in the mantle, *Nature,* **446,** 787–790.

Kohlstedt, D., 2007. Properties of rocks and minerals - constitutive equations, rheological behavior, and viscosity of rocks, in *Treatise on Geophysics,* Vol. 2, pp. 389–417, ed. Price, G., Elsevier, Oxford.

Kohlstedt, D. & Wang, Z., 2001. Grain-boundary sliding accomodated dislocation creep in dunite, *EOS, Trans. Am. geophys. Un.,* **82**(47), F1137.

Kohlstedt, D. & Weathers, M., 1980. Deformation-induced microstructures paleopiezometers and differential stress in deeply eroded fault zones, *J. geophys. Res.,* **85**(11), 6269–6285.

Korenaga, J. & Karato, S.-I., 2008. A new analysis of experimental data on olivine rheology, *J. geophys. Res.,* **113,** B02403, doi:10.1029/2007JB005100.

Landuyt, W. & Bercovici, D., 2009. Formation and structure of lithospheric shear zones with damage, *Phys. Earth planet. Inter.,* **175,** 115–126.

Langdon, T., 2006. Grain boundary sliding revisited: Developments in sliding over four decades, *J. Mater. Sci.,* **41,** 597–609.

Leloup, P.H., Ricard, Y., Battaglia, J. & Lacassin, R., 1999. Shear heating in continental strike-slip shear zones: model and field examples, *Geophys. J. Int.,* **136,** 19–40.

Lifshitz, I.M. & Slyozov, V.V., 1961. The kinetics of precipitation from supersaturated solid solutions, *J. Phys. Chem. Solids,* **19,** 35–50.

Montési, L. & Zuber, M., 2002. A unified description of localization for application to large-scale tectonics, *J. geophys. Res.,* **107**(B3).

Montési, L.G.J. & Hirth, G., 2003. Grain size evolution and the rheology of ductile shear zones: from laboratory experiments to postseismic creep, *Earth planet. Sci. Lett.,* **211,** 97–110.

Ogawa, M., 2003. Plate-like regime of a numerically modeled thermal convection in a fluid with temperature-, pressure-, and stress-history-dependent viscosity, *J. geophys. Res.,* **108,** 2067, doi:10.1029/2000JB000069.

Post, R.L., 1977. High-temperature creep of mt burnet-dunite, *Tectonophysics,* **42,** 75–110.

Ranalli, G., 1995. *Rheology of the Earth,* 2nd edn, Chapman and Hall, London, UK.

Raterron, P., Wu, Y., Weidner, D. & Chen, J., 2004. Low-temperature olivine rheology at high pressure, *Phys. Earth planet. Inter.,* **145,** 149–159.

Reuss, E., 1930. Beruecksichtigung der elastischen formaenderungen in der plastizitaetstheorie, *Zeits. angew. Math. Mech. (ZAMM),* **10,** 266–274.

Ricard, Y. & Bercovici, D., 2009. A continuum theory of grain size evolution and damage, *J. geophys. Res.,* **114,** B01204, doi:10.1029/2007JB005491.

Ross, J., Lallemant, H.A. & Carter, N., 1980. Stress dependence of recrystallized-grain and subgrain size in olivine, *Tectonophysics,* **70,** 39–61.

Shimizu, I., 1998a. Lognormality of crystal size distribution in dynamic recrystallization, *Forma,* **13,** 1–11.

Shimizu, I., 1998b. Stress and temperature dependence of recrystallized grain size: a subgrain misorientation model, *Geophys. Res. Lett.,* **25,** 4237–4240.

Shimizu, I., 1999. A stochastic model of grain size distribution during dynamic recrystallization, *Phil. Mag.,* **A79,** 1217–1231.

Shimizu, I., 2008. Theories and applicability of grain size piezometers: the role of dynamic recrystallization mechanisms, *J. Struct. Geol.,* **30,** 899–917.

Slotemaker, A.K., 2006. Dynamic recrystallization and grain growth in olivine rocks, *PhD thesis,* Utrecht University, Utrecht.

Stein, C., Schmalzl, J. & Hansen, U., 2004. The effect of rheological parameters on plate behaviour in a self-consistent model of mantle convection, *Phys. Earth planet. Inter.,* **142,** 225–255.

Stipp, M., Tullis, J., Scherwath, M. & Behrmann, J., 2010. A new perspective on paleopiezometry: dynamically recrystallized grain size distributions indicate mechanism changes, *Geology,* **38**(8), 759–762.

Tackley, P.J., 2000. Self consistent generation of tectonic plates in time-dependent, three dimensional mantle convection simulations, *Geochem. Geophys. Geosyst.,* **1**(8), doi:10.1029/2000GC000036.

Tommasi, A., Knoll, M., Vauchez, A., Signorelli, J., Thoraval, C. & Loge, R., 2009. Structural reactivation in plate tectonics controlled by olivine crystals anisotropy, *Nat. Geosci.,* **2,** 423–427.

Twiss, R., 1977. Theory and applicability of a recrystallized grain size paleopiezometer, *Pure appl. Geophys.,* **115,** 227–244.

Van der Wal, D., Chopra, P., Drury, M.R. & Fitzgerald, J.D., 1993. Relationships between dynamically recrystallized grain size and deformation conditions in experimentally deformed olivine rocks, *Geophys. Res. Lett.,* **20,** 1479–1482.

Wagner, C., 1961. Theory der alterung von niederschlaegen durch umloesen (oswald reifung), *Zeitschr. Elektrochemie,* **65,** 581–591.

Weinstein, S.A. & Olson, P.L., 1992. Thermal convection with non-newtonian plates, *Geophys. J. Int.,* **111,** 515–530.

Zhang, S., Karato, S.-I., FitzGerald, J., Faul, U. & Zhou, Y., 2000. Simple shear deformation of olivine aggregates, *Tectonophysics,* **316,** 133–152.